Third-order Time Integration Scheme for Structural Dynamics

Eva Zupan
HSE, Ljubljana, Slovenia
and University of Ljubljana
Faculty of Civil and Geodetic Engineering
Ljubljana, Slovenia
Email: eva.zupan.lj@gmail.com

Dejan Zupan
University of Ljubljana
Faculty of Civil and Geodetic Engineering
Ljubljana, Slovenia
Email: dejan.zupan@fgg.uni-lj.si

***Abstract*—In this paper, we propose a new time integration scheme for rigid and flexible body dynamics, where rotational degrees of freedom are incorporated into the model. To properly consider the multiplicative and non-commutative nature of three-dimensional rotations, the integration scheme is designed in a special way. It employs the representation of rotations with quaternions and quaternion exponential to preserve the orthogonality condition. The scheme is implicit and its accuracy is of the third order. To gain the desired order of the scheme for rotational degrees of freedom, an additional correction function is introduced that compensates the non-commutativity of rotations. The performance of the scheme is demonstrated by several examples.**

Keywords–time integrators; three-dimensional rotations; quaternions; dynamics.

I. INTRODUCTION

Problems in structural dynamics can be very demanding. The differential equations that govern the problem are often stiff and the configuration space usually consists of three-dimensional rotations. Because the spatial rotations are elements of the multiplicative $\mathcal{SO}(3)$ group, the configuration space becomes a non-linear manifold. Thus, numerical solution methods need to be specially designed to properly consider non-commutativity and non-additivity of three-dimensional rotations. Simo and Vu-Quoc [1] proposed an adjustment of the implicit Newmark method to treat the spatial rotations. Their method is of second order and can be considered a special case of the methods on Lie groups, later presented by Munthe-Kaas [2]. The crucial idea employed in [1] and [2] is to approximate the update in the tangent space and map it onto the configuration space via an exponential function. However, the non-commutativity of rotations demands the construction of correction functions when higher orders of approximation are desired.

After introducing a basis into the three-dimensional Euclidean space, members of $\mathcal{SO}(3)$ group are represented by orthogonal 3×3 matrices. The orthogonality condition introduces six constraints to their components and their treatment is highly important, see e.g., [3]. It seems natural to choose a three-component parametrization of rotations, but no such parametrization is free from singularities. A promising alternative, employed here, is the algebra of quaternions [4]. Quaternions are members of a four dimensional space, therefore a single scalar constraint needs to be satisfied in the quaternion representation of rotations. It was only recently that novel quaternion-based rigid and flexible-body dynamic formulations were proposed, see [5]-[7]. All these approaches treat the unity constraint of rotational quaternions as a member of the governing equations of the problem. This allows the use of standard time integration methods, but increases the computational demands.

In the present paper, we therefore develop a time integration scheme of third-order that is properly adapted to quaternion representation of rotations. Our scheme exactly preserves the unit norm constraint of rotational quaternions following the approach of Munthe-Kaas [2] and Zanna [8] and adopts it to quaternion algebra. The correction function needed to compensate the non-commutativity is derived to introduce an implicit time integration scheme of the third order. The proposed method consists of two implicit stages of second order followed by an explicit third-order step, which allows local error control without any additional computational costs.

The rest of the paper is structured as follows. Section II introduces some primary definitions. In Section III, we describe a novel time integration method for dynamic problems. Numerical examples are presented in Section IV. The paper ends with concluding remarks.

II. PRIMARY DEFINITIONS

Two orthogonal reference frames are introduced (see Figure 1):

(i) a *reference frame* with a reference point $\mathcal{O}$ and a set of fixed orthonormal base vectors $\left\{\vec{g}_1, \vec{g}_2, \vec{g}_3\right\}$, and

(ii) a *body frame* rigidly attached to the body defined by three orthonormal base vectors $\left\{\vec{G}_1(t), \vec{G}_2(t), \vec{G}_3(t)\right\}$.

The body frame is at an arbitrary time, t, uniquely defined by the position vector $\vec{r}(t)$ of its origin and by the rotation between the base vectors $\left\{\vec{g}_1, \vec{g}_2, \vec{g}_3\right\}$ and $\left\{\vec{G}_1(t), \vec{G}_2(t), \vec{G}_3(t)\right\}$. Here, we employ rotational quaternions to parametrize the rotations. Using the algebra of quaternions, the relation between the moving and the fixed basis is written as

$$\vec{G}_i(t) = \widehat{q}(t) \circ \vec{g}_i \circ \widehat{q}^*(t), \qquad i = 1, 2, 3, \tag{1}$$

where $\widehat{q}$ is the rotational quaternion, $\widehat{q}^*$ is the conjugated quaternion, and $(\circ)$ denotes the quaternion product.

The set of quaternions $\mathbb{H}$ is a four-dimensional Euclidean space. Quaternions can be described as the sum of a scalar and a vector: $\widehat{x} = s + \vec{v} = \left(s, \vec{v}\right)$, $s \in \mathbb{R}$, $\vec{v} \in \mathbb{R}^3$. Addition

 ISBN: 978-1-61208-599-9

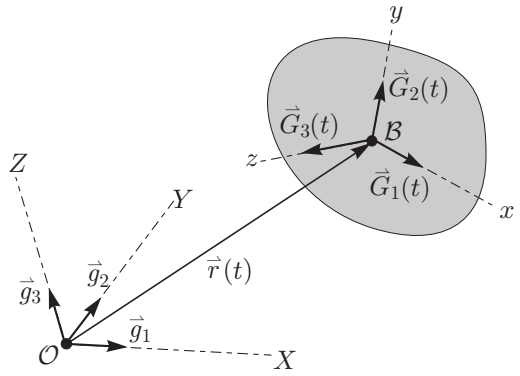

Figure 1. Base vectors.

and scalar multiplication are inherited from $I\!R^4$, while the *quaternion multiplication* is defined as:

$$\widehat{x} \circ \widehat{y} = \left(s\,c - \vec{v} \cdot \vec{w}\right) + \left(c\vec{v} + s\vec{w} + \vec{v} \times \vec{w}\right), \qquad (2)$$

where $\widehat{y} = c + \vec{w} \in I\!H$ and $(\cdot)$ and $(\times)$ are the scalar and the cross-vector product, respectively. The quaternion multiplication is associative but it is not commutative, which makes the set of quaternions an associative non-commutative algebra over $I\!R$. In what follows, abstract elements of $I\!R^3$ and $I\!H$ will be replaced by one-column representations and will be denoted by bold face symbols. The additional base vector of quaternion space is taken to be the identity element $\widehat{1} = 1 + \vec{0}$. An arbitrary quaternion, $\widehat{x} = s + \vec{v}$, can thus be expressed with respect to either of the two bases

$$\widehat{x} = s\,\widehat{1} + v_1\,\vec{g}_1 + v_2\,\vec{g}_2 + v_3\,\vec{g}_3 = S\,\widehat{1} + V_1\vec{G}_1 + V_2\vec{G}_2 + V_3\vec{G}_3$$

and the components are gathered in one-column matrices. For a more detailed presentation of the quaternion algebra, the reader is referred to the textbook [4].

The differentiation of quantities with respect to time t is essential for dynamics. To describe the rate of change of the position vector, we introduce

$$\mathbf{v} = \dot{\mathbf{r}}, \qquad (3)$$

describing the *velocity* in the global frame. The differentiation of equation (1) with respect to t gives a measure for the rate of change of the local basis:

$$\mathbf{\Omega} = 2\widehat{\mathbf{q}}^{*} \circ \dot{\widehat{\mathbf{q}}}, \qquad (4)$$

where $\mathbf{\Omega}$ denotes the *angular velocity* with respect to the local basis. Furthermore, we define acceleration as $\mathbf{a} = \dot{\mathbf{v}}$ and angular acceleration as $\boldsymbol{\alpha} = \dot{\mathbf{\Omega}}$.

As they are a part of many engineering problems, spatial rotations often need to be reconstructed from the prescribed, measured or assumed angular velocity field, i.e., an efficient solution for equation (4) is desired. For the special case of constant angular velocity, a closed form analytical solution of the initial value problem

$$\dot{\widehat{\mathbf{q}}}\,(t) = \frac{1}{2}\,\widehat{\mathbf{q}}\,(t) \circ \mathbf{\Omega}, \qquad \widehat{\mathbf{q}}\,(t_0) = \widehat{\mathbf{q}}_0, \qquad (5)$$

can be found. It reads

$$\widehat{\mathbf{q}}\,(t) = \widehat{\mathbf{q}}_0 \circ \exp\left(\frac{t}{2}\overline{\mathbf{\Omega}}\right), \qquad (6)$$

where the *quaternion exponential* exp is defined by infinite power series:

$$\exp\left(\widehat{\mathbf{x}}\right) = \sum_{k=1}^{\infty} \frac{\widehat{\mathbf{x}}^k}{1!} = \widehat{\mathbf{1}} + \frac{\widehat{\mathbf{x}}}{1!} + \frac{1}{2!}\widehat{\mathbf{x}} \circ \widehat{\mathbf{x}} + \frac{1}{3!}\widehat{\mathbf{x}} \circ \widehat{\mathbf{x}} \circ \widehat{\mathbf{x}} + \ldots. \qquad (7)$$

The result (6) indicates that the exponential map may also be a suitable choice for the approximation of the general solution. We need to point out that, without some additional effort, its direct use results in only second-order approximations of the exact solution. The details are presented in [9].

After we introduce the rotational vector $\boldsymbol{\vartheta} = \vartheta\mathbf{n}$, where ϑ is the angle of rotation and $\mathbf{n}$ denotes the unit vector on the axis of rotation, any rotational quaternion can also be expressed as

$$\widehat{\mathbf{q}}\,(\boldsymbol{\vartheta}) = \cos\frac{\vartheta}{2} + \sin\frac{\vartheta}{2}\,\frac{\boldsymbol{\vartheta}}{\vartheta}, \qquad (8)$$

which gives a firm physical meaning to its components.

III. Time discretization

To solve the set of differential equations of a moving body, a third-order integration scheme is proposed. Since the equations we are dealing with are often stiff, we stem from the well known combination of trapezoidal rule and backward differentiation formula (TR-BDF2 method) [10], adopt it to differential equations of the second order and extend it to properly consider the rotational degrees of freedom. The TR-BDF2 scheme consists of three-stages: the first two stages are implicit schemes of second order while the third stage is explicit and of the third order of accuracy. The corresponding Butcher array [10] reads

$$\begin{array}{c|lll} 0 & 0 & 0 & 0 \\ \tau & \tau/2 & \tau/2 & 0 \\ 1 & w & w & \tau/2 \\ \hline & w & w & \tau/2 \\ \hline & (2-\tau)/6 & (3\tau+2)/6 & \tau/6 \end{array}, \qquad (9)$$

where $\tau = 2 - \sqrt{2}$ and $w = \frac{\sqrt{2}}{4}$. The difference between the formulae of third and second order allows the local error control without any additional computational costs.

The scheme (9) is adopted here to solve the equations of dynamic equilibrium. Average velocities and average angular velocities between the two successive times are chosen as the primary iterative unknowns of the scheme. Such a choice is especially important for rotational degrees of freedom since the angular velocities, when expressed with respect to the moving basis, are additive. This property simplifies the linearization and update procedure needed in implicit schemes on non-linear configuration spaces. A detailed description of each stage of the proposed scheme will be presented in the sequel. To indicate that a particular quantity $(\cdot)$ is evaluated at a time t_m we employ the notation: $(\cdot)^{[m]}$.

 ISBN: 978-1-61208-599-9

A. First stage

Let us assume that the configuration of a moving body is known at the discrete time t_n. The size of a current time step is denoted by h. The first stage gives the approximation of kinematic quantities at the intermediate time $t_{n+\tau} = t_n + \tau h$. Directly from the trapezoidal rule, we have:

$$\overline{\mathbf{v}} = \frac{\mathbf{v}^{[n]} + \mathbf{v}^{[n+\tau]}}{2} = \frac{\mathbf{r}^{[n+1]} - \mathbf{r}^{[n]}}{\tau h}, \tag{10}$$

which yields

$$\mathbf{r}^{[n+\tau]} = \mathbf{r}^{[n]} + \tau h \overline{\mathbf{v}}.$$

An analogous formula can be used for linear accelerations:

$$\frac{\mathbf{a}^{[n]} + \mathbf{a}^{[n+\tau]}}{2} = \frac{\mathbf{v}^{[n+\tau]} - \mathbf{v}^{[n]}}{\tau h}.$$

The average velocity $\overline{\mathbf{v}}$ is chosen to be the iterative unknown of the scheme while the remaining quantities are expressed with the values at the current time t_n and $\overline{\mathbf{v}}$. This gives

$$\begin{aligned} \mathbf{r}^{[n+\tau]} &= \mathbf{r}^{[n]} + \tau h \overline{\mathbf{v}} \\ \mathbf{v}^{[n+\tau]} &= -\mathbf{v}^{[n]} + 2\overline{\mathbf{v}} \\ \mathbf{a}^{[n+\tau]} &= -\mathbf{a}^{[n]} - \frac{4}{\tau h}\mathbf{v}^{[n]} + \frac{4}{\tau h}\overline{\mathbf{v}}. \end{aligned} \tag{11}$$

A similar approach can be used for rotational degrees of freedom, however the relation between rotational quaternions and angular velocities is based on the result (6) which preserves the configuration space and is second-order accurate. The corresponding scheme then reads

$$\begin{aligned} \widehat{\mathbf{q}}^{[n+\tau]} &= \widehat{\mathbf{q}}^{[n]} \circ \exp\left(\frac{\tau h}{2}\overline{\boldsymbol{\Omega}}\right) \\ \boldsymbol{\Omega}^{[n+\tau]} &= -\boldsymbol{\Omega}^{[n]} + 2\overline{\boldsymbol{\Omega}} \\ \boldsymbol{\alpha}^{[n+\tau]} &= -\boldsymbol{\alpha}^{[n]} - \frac{4}{\tau h}\boldsymbol{\Omega}^{[n]} + \frac{4}{\tau h}\overline{\boldsymbol{\Omega}}, \end{aligned} \tag{12}$$

where $\overline{\boldsymbol{\Omega}}$ denotes the average angular velocity vector

$$\overline{\boldsymbol{\Omega}} = \frac{\boldsymbol{\Omega}^{[n]} + \boldsymbol{\Omega}^{[n+\tau]}}{2}, \tag{13}$$

which is taken to be the iterative unknown of the scheme.

Two possible predictors of the first stage seem natural: (i) $\mathbf{v}_0^{[n+\tau]} = \mathbf{v}^{[n]}$ and $\boldsymbol{\Omega}_0^{[n+\tau]} = \boldsymbol{\Omega}^{[n]}$ or (ii) $\mathbf{a}_0^{[n+\tau]} = \mathbf{a}^{[n]}$ and $\boldsymbol{\alpha}_0^{[n+\tau]} = \boldsymbol{\alpha}^{[n]}$. The first one was found unsuitable as it sometimes leads to the instability of long-term numerical calculations. Therefore, the second predictor, based on the accelerations from the previous time step, is used here. The initial guess for the remaining quantities then follows directly from (11)–(12)

B. Second stage

The second stage is based on second order approximation at time t_{n+1} using the configuration values at times t_n and $t_{n+\tau}$. The third line of (9) gives:

$$\begin{aligned} \mathbf{r}^{[n+1]} &= \mathbf{r}^{[n]} + h\left(w\mathbf{v}^{[n]} + w\mathbf{v}^{[n+\tau]} + \frac{\tau}{2}\mathbf{v}^{[n+1]}\right) \\ \mathbf{v}^{[n+1]} &= \mathbf{v}^{[n]} + h\left(w\mathbf{a}^{[n]} + w\mathbf{a}^{[n+\tau]} + \frac{\tau}{2}\mathbf{a}^{[n+1]}\right). \end{aligned}$$

We now use the notation

$$\overline{\mathbf{v}} = w\mathbf{v}^{[n]} + w\mathbf{v}^{[n+\tau]} + \frac{\tau}{2}\mathbf{v}^{[n+1]} \tag{14}$$

and treat $\overline{\mathbf{v}}$ as the primary iterative unknown. The second stage expressed with $\overline{\mathbf{v}}$ now reads:

$$\begin{aligned} \mathbf{r}^{[n+1]} &= \mathbf{r}^{[n]} + h\overline{\mathbf{v}} \\ \mathbf{v}^{[n+1]} &= -\frac{2w}{\tau}\left(\mathbf{v}^{[n]} + \mathbf{v}^{[n+\tau]}\right) + \frac{2}{\tau}\overline{\mathbf{v}} \\ \mathbf{a}^{[n+1]} &= -\frac{2w}{\tau}\left(\mathbf{a}^{[n]} + \mathbf{a}^{[n+\tau]}\right) \\ &\quad - \frac{4}{\tau^2 h}\left(\left(w + \frac{\tau}{2}\right)\mathbf{v}^{[n]} + w\mathbf{v}^{[n+\tau]}\right) + \frac{4}{\tau^2 h}\overline{\mathbf{v}}. \end{aligned} \tag{15}$$

Analogous scheme for rotational degrees of freedom is obtained by considering (6):

$$\begin{aligned} \widehat{\mathbf{q}}^{[n+\tau]} &= \widehat{\mathbf{q}}^{[n]} \circ \exp\left(\frac{h}{2}\overline{\boldsymbol{\Omega}}\right) \\ \boldsymbol{\Omega}^{[n+\tau]} &= -\frac{2w}{\tau}\left(\boldsymbol{\Omega}^{[n]} + \boldsymbol{\Omega}^{[n+\tau]}\right) + \frac{2}{\tau}\overline{\boldsymbol{\Omega}} \\ \boldsymbol{\alpha}^{[n+\tau]} &= -\frac{2w}{\tau}\left(\alpha^{[n]} + \alpha^{[n+\tau]}\right) \\ &\quad - \frac{4}{\tau^2 h}\left(\left(w + \frac{\tau}{2}\right)\boldsymbol{\Omega}^{[n]} + w\boldsymbol{\Omega}^{[n+\tau]}\right) + \frac{4}{\tau^2 h}\overline{\boldsymbol{\Omega}}, \end{aligned} \tag{16}$$

where

$$\overline{\boldsymbol{\Omega}} = w\boldsymbol{\Omega}^{[n]} + w\boldsymbol{\Omega}^{[n+\tau]} + \frac{\tau}{2}\boldsymbol{\Omega}^{[n+1]}. \tag{17}$$

From the known values at t_n and $t_{n+\tau}$ we can evaluate a better predictor for the second stage. A cubic Hermit interpolation, see, e.g., [11], of velocities and angular velocities trough t_n and $t_{n+\tau}$ yields

$$\begin{aligned} \mathbf{v}_0^{[n+1]} &= \mathbf{v}^{[n]} + \frac{2-3\tau}{\tau^3}\left(\mathbf{v}^{[n]} - \mathbf{v}^{[n+\tau]}\right) \\ &\quad + \frac{h\,(1-\tau)}{\tau^2}\left((1-\tau)\,\mathbf{a}^{[n]} + \mathbf{a}^{[n+\tau]}\right) \\ \boldsymbol{\Omega}_0^{[n+1]} &= \boldsymbol{\Omega}^{[n]} + \frac{2-3\tau}{\tau^3}\left(\boldsymbol{\Omega}^{[n]} - \boldsymbol{\Omega}^{[n+\tau]}\right) \\ &\quad + \frac{h\,(1-\tau)}{\tau^2}\left((1-\tau)\,\boldsymbol{\alpha}^{[n]} + \boldsymbol{\alpha}^{[n+\tau]}\right). \end{aligned}$$

C. Third stage

Finally, we use an explicit third-order scheme to increase the accuracy of the results at time t_{n+1}. For the position vector, we can directly employ the last line of Butcher's array (9), which gives

$$\mathbf{r}^{[n+1]} = \mathbf{r}^{[n]} + h\left(\frac{1-w}{3}\mathbf{v}^{[n]} + \frac{3w+1}{3}\mathbf{v}^{[n+\tau]} + \frac{\tau}{6}\mathbf{v}^{[n+1]}\right). \tag{18}$$

Analogous formula for rotational degrees of freedom can be written as

$$\begin{aligned} \widehat{\mathbf{q}}^{[n+1]} = \widehat{\mathbf{q}}^{[n]} \circ \exp\Big(&\mathrm{Corr} \\ &+ \frac{h}{2}\left(\frac{1-w}{3}\boldsymbol{\Omega}^{[n]} + \frac{3w+1}{3}\boldsymbol{\Omega}^{[n+\tau]} + \frac{\tau}{6}\boldsymbol{\Omega}^{[n+1]}\right)\Big), \end{aligned} \tag{19}$$

where the correction term Corr is needed to gain the third order of accuracy. Thus, the correction term is determined in such a way that (19) agrees with the analytical solution of Eq. (5) up to the third order. After a lenghty derivation and taking into account the analytical solution presented in [9], we get

$$\mathrm{Corr} = \frac{h^2}{48\tau\,(\tau-1)}\,\boldsymbol{\Omega}^{[n]} \times \left(\tau^2\boldsymbol{\Omega}^{[n+1]} - \boldsymbol{\Omega}^{[n+\tau]}\right). \tag{20}$$

 ISBN: 978-1-61208-599-9

In contrast to the previous two stages, velocities and angular velocities are left unchanged since their higher order approximation quickly amplifies stiff components of the system and the convergence of the method deteriorates.

IV. NUMERICAL STUDIES

We will demonstrate the performance of the proposed method on several numerical examples. Quadratic convergence of Newton iteration scheme was achieved in all examples due to consistent linearization of equations with proper consideration of rotational degrees of freedom.

A. Rotating body under prescribed torque

In the first set of examples, we consider a rotating rigid body subjected only to the analytically prescribed external torque $\boldsymbol{M}$. Equations of motion are then as follows

$$\mathbf{J}\dot{\boldsymbol{\Omega}} + \boldsymbol{\Omega} \times \mathbf{J}\boldsymbol{\Omega} = \widehat{\mathbf{q}}^{*} \circ \boldsymbol{M} \circ \widehat{\mathbf{q}}, \tag{21}$$

where $\mathbf{J}$ is the inertia matrix. When equation (21) is evaluated at discrete time t_{n+1} and the proposed time discretization is taken into account, the average velocities and angular velocities, $\overline{\mathbf{v}}$ and $\overline{\boldsymbol{\Omega}}$, become the only unknowns of the problem. The obtained time-discrete equations are non-linear and are therefore solved iteratively.

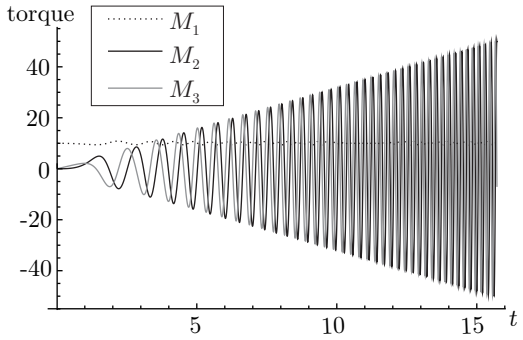

Figure 2. The torque applied to the rigid body. Load case (i).

We base this test on the assumed analytical field of rotations, i.e., the components of the rotational vector are known analytical functions of time. From (5), (8) and (21) we obtain the analytical expression for the applied torque $\boldsymbol{M}$ and the initial values $\widehat{\mathbf{q}}_0 = \widehat{\mathbf{q}}\,(0)$ and $\boldsymbol{\Omega}^{[0]} = \boldsymbol{\Omega}\,(0)$. We employed Mathematica [12] for these symbolic manipulations. From the numerically obtained rotational quaternions the discrete numerical solution in terms of rotational vectors is evaluated using the Spurrier algorithm [13]. Numerical results are then compared to the exact ones.

Two cases are considered for which the rotational vectors are: (i) the quadratic function: $\boldsymbol{\vartheta}\,(t) = \left[t^2, 0, t/5\right]^T$ and (ii) the harmonic function: $\boldsymbol{\vartheta}\,(t) = \left[t + \sin(t), 0, \cos(t)\right]^T$ of time. The inertia tensor with respect to the principal axes of the rotating body was taken to be $\mathbf{J} = \mathrm{diag}\,(5, 5, 1)$. The results were obtained on the time interval $[0, 5\pi]$ using the present method and in the field of structural dynamics widely used Newmark algorithm for $SO\,(3)$ by Simo and Vu-Quoc [1]. The absolute errors of the norm of rotational vector, i.e., the absolute errors of the angle of rotation are presented and compared.

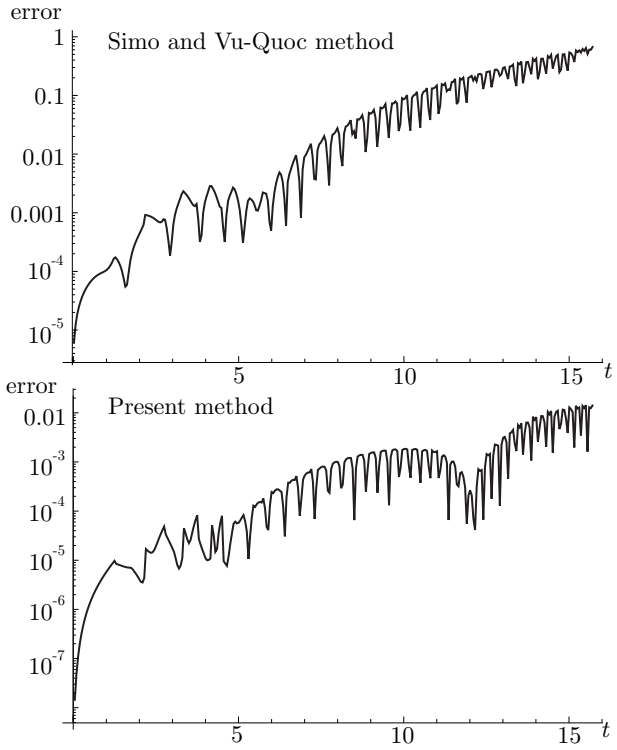

Figure 3. Load case (i). Absolute error of the angle of rotation for the time step $h = 0.05$.

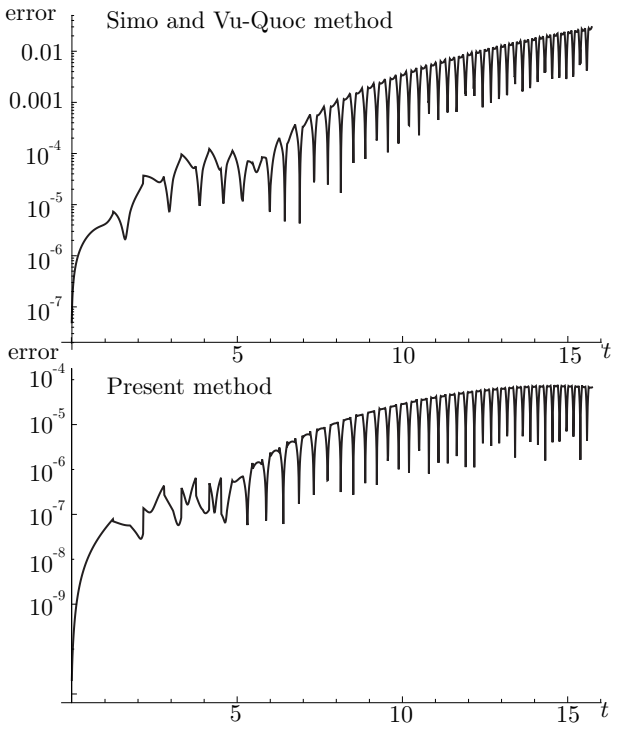

Figure 4. Load case (i). Absolute error of the angle of rotation for the time step $h = 0.01$.

The applied torque for the first load case is presented in Figure 2. The magnitude of the torque is increasing with time

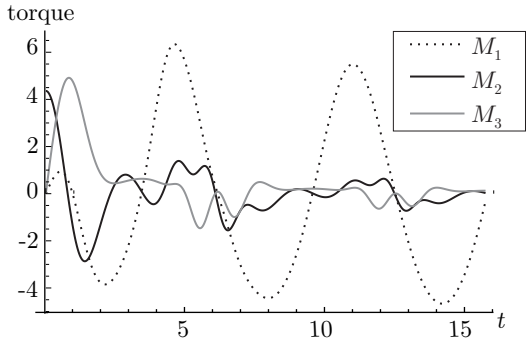

Figure 5. The torque applied to the rigid body. Load case (ii).

and oscilating with increasing frequency, which makes this example quite challenging. For the longer time step $h = 0.05$, the absolute errors between the exact and numerically obtained angle of rotation are shown in Figure 3. Note that the graphs are presented in the logarithmic scale. The higher order of accuracy of the proposed method is evident. This observation is additionally confirmed when smaller time step $h = 0.01$ is taken, see Figure 4. Again, the proposed method is advantageous compared to the widely used method by Simo and Vu-Quoc [1]. As expected, the absolute error is increasing with time, but the higher order of local accuracy of the proposed method results in much smaller global errors.

The applied torque for the second load case is shown in Figure 5. For this load case, the magnitude of the torque is not increasing, but we still cannot avoid the accumulation of the error with large number of time steps.

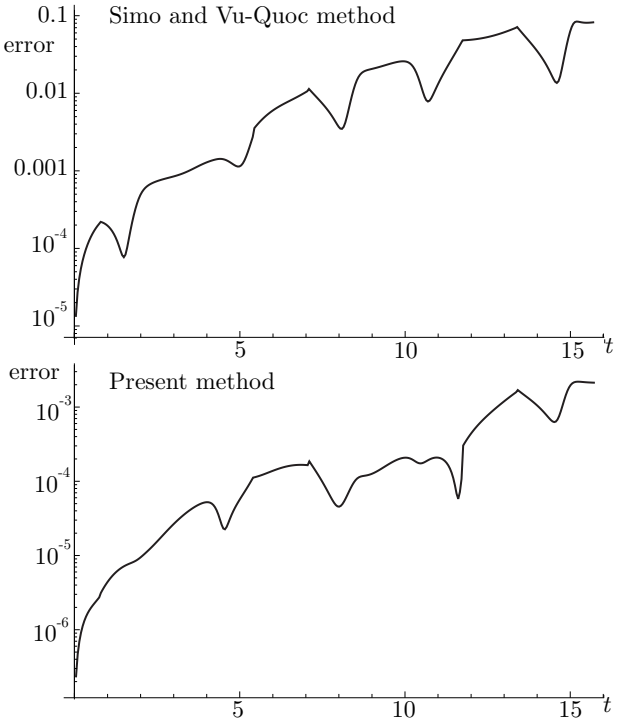

Figure 6. Load case (ii). Absolute error of the angle of rotation for the time step $h = 0.05$.

The results presented in Figure 6 were obtained using time step $h = 0.05$. The maximum absolute error of the second-order method was 0.084, while the proposed method is more accurate with the maximum global error being 0.0022. The accuracy is considerably improved by reducing the time step. When $h = 0.01$, the maximum absolute error of Simo and Vu-Quoc method [1] is 0.0035, while for the present method it is no more than 0.000017.

B. Large deflections of right-angle cantilever

This classical benchmark problem for frame-like structures was introduced by Simo and Vu-Quoc [1]. A right-angle cantilever beam is subjected to a triangular pulse out-of-plane load at the elbow, see Figure 7. After the removal of the external force, the cantilever undergoes free vibrations. Each part of the cantilever is dicretized with five third-order beam elements. Details on the finite elements used are presented in [14]. Both time integrators are employed to obtain the solution. A dynamic response of the cantilever involves very large magnitudes of displacements and rotations together with finite strains. The centroidal mass-inertia matrix of the cross-section is diagonal: $\mathbf{J}_\rho = \mathrm{diag}\,[\ 20 \quad 10 \quad 10\ ]$.

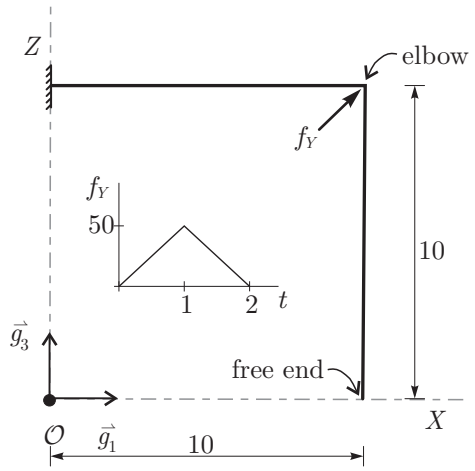

Figure 7. The right-angle cantilever subjected to out-of-plane loading.

The dynamic response of the beam was computed on the time interval $[0, 4]$ with different time steps. Since no analytical solution exists for this problem, the solution obtained with very small time step $h = 0.00025$ was taken as the reference one.

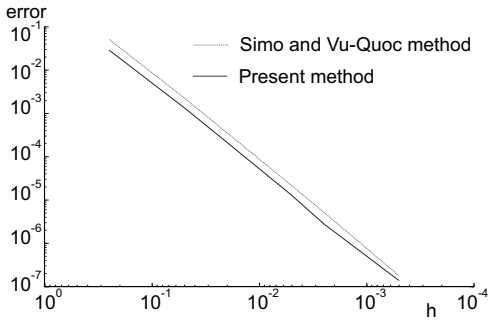

Figure 8. Right-angle cantilever: logarithmic plot of the displacement errors at the elbow.

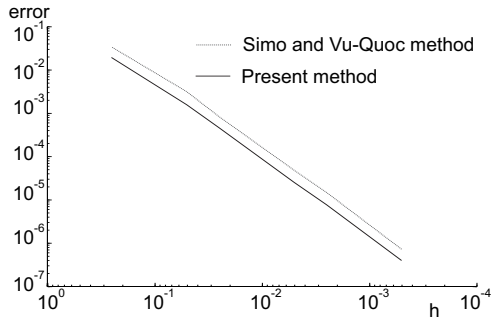

Figure 9. Right-angle cantilever: logarithmic plot of the rotation errors at the elbow.

Figures 8 and 9 present the convergence plots of the results at the elbow. Note that the proposed method gives more accurate results than the scheme by Simo and Vu-Quoc. The difference is evident but not as high as for the rigid body motion. The main reason for this lies in the approximation of strain vectors, which was taken the same for both integrators and limits the benefits of the proposed method.

V. Conclusion

We have presented a third order time integrator for rigid and flexible body dynamics. The proposed scheme is consistent with the properties of three-dimensional rotations and allows the rotational degrees of freedom to be treated with the same accuracy as the translational ones. An additional benefit is the local error control without any additional computational demands. To achieve an additional order of accuracy, two implicit and one explicit step are needed in our approach. This means that by doubling the computational costs we gain one order of accuracy and free local error control without any additional computational time needed in contrast to second-order schemes, where local error control demands additional evaluations. The proposed method is thus competitive among implicit methods for rigid body dynamics. The influence of the strain approximation on flexible beam dynamics will be the subject of further research.

Acknowledgment

This work was supported by the Slovenian Research Agency through the research programme P2-0260 and the research project J2-8170. The support is gratefully acknowledged.

References

[1] J. C. Simo and L. Vu-Quoc, “On the dynamics in space of rods undergoing large motions - a geometrically exact approach,” Comput. Meth. Appl. Mech. Eng., vol. 66, no. 2, 1988, pp. 125–161.

[2] H. Munthe-Kaas, “Runge-Kutta methods on Lie groups,” Bit, vol. 38, no. 1, 1998, pp. 92–111.

[3] O. A. Bauchau and L. Trainelli, “The vectorial parameterization of rotation,” Nonlinear Dyn., vol. 32, no. 1, 2003, pp. 71–92.

[4] J. P. Ward, Quaternions and Cayley Numbers, Kluwer Academic Publishers, Dordrecht–Boston–London, 1997.

[5] P. Betsch and R. Siebert, “Rigid body dynamics in terms of quaternions: Hamiltonian formulation and conserving numerical integration,” Int. J. Numer. Methods Eng., vol. 79, no. 4, 2009, pp. 444–473.

[6] H. Lang, J. Linn, and M. Arnold, “Multi-body dynamics simulation of geometrically exact Cosserat rods,” Multibody Syst. Dyn., vol. 25, no. 3, 2011, pp. 285–312.

[7] E. Zupan, M. Saje, and D. Zupan, “Dynamics of spatial beams in quaternion description based on the Newmark integration scheme,” Comput. Mech., vol. 51, no. 1, 2013, pp. 47–64.

[8] A. Zanna, “Collocation and relaxed collocation for the FER and the Magnus expansions,” SIAM J. Numer. Anal., vol. 36, no. 4, 1999, pp. 1145–1182.

[9] E. Zupan and D. Zupan, “On higher order integration of angular velocities using quaternions,” Mech. Res. Commun., vol. 55, 2014, pp. 77–85.

[10] M. E. Hosea and L. F. Shampine, “Analysis and implementation of TR-BDF2,” Appl. Numer. Math., vol. 20, no. 1-2, 1996, pp. 21–37.

[11] R. L. Burden, J. D. Faires, Numerical analysis, Brooks/Cole, 1997.

[12] Wolfram Research, Inc., “Mathematica, Version 10.2,” 2015, Champaign, Illinois.

[13] R. A. Spurrier, “Comment on singularity-free extraction of a quaternion from a direction-cosine matrix,” J. Spacecr. Rockets, vol. 15, no. 4, 1978, p. 255.

[14] E. Zupan and D. Zupan, “Velocity-based approach in non-linear dynamics of three-dimensional beams with enforced kinematic compatibility,” Comput. Meth. Appl. Mech. Eng., vol. 310, 2016, pp. 406–428.

 ISBN: 978-1-61208-599-9